ISSN 1070-3284, Russian Journal of Coordination Chemistry, 2018, Vol. 44, No. 9, pp. 540–546. © Pleiades Publishing, Ltd., 2018.

Structural Diversity of Two Coordination Polymers Based on Bis(4-(1*H*-Imidazol-1-Yl)phenyl)methanone and Polycarboxylate Coligands: Syntheses, Structures, and Fluorescent Properties[1]

G. F. Wang*

Department of Applied Chemistry, Yuncheng University, Yuncheng, 044000 P.R. China

**e-mail: ycuwgf@163.com*

Received October 10, 2017

Abstract—Two novel coordination polymers, $[Zn_2(Bipmo)_2(Adip)_2 \cdot 2H_2O]_n$ (**I**), $[Zn(Bipmo)(Adip) \cdot 2H_2O]_n$ (**II**) (Bipmo = bis(4-(1*H*-imidazol-1-yl)phenyl)methanone, H_2Adip = adipic acid) with unprecedented structures, have been synthesized and structurally characterized. by single-crystal X-raydiffraction (CIF files CCDC nos. 1555292 (**I**), 1555289 (**II**)). Complex **I** exhibits 4-fold interpenetrating wave-like sheets, which interpenetrate in a 2D → 2D parallel manner and pillar to generate 3D architectures. Complex **II** consists of a 2-fold 4-connected 3D coordination polymers network with a point symbol of $(6^5.8)$. The results indicate that the central metal ions, polycarboxylate and semirigid co-ligands have a great effect on the formation and the structures of the coordination polymers. Moreover, the thermal stability and the luminescent properties of complexes **I**, **II** were investigated.

Keywords: coordination polymers, inorganic-organic hybrids, semirigid ligand, topology, crystal structure

DOI: 10.1134/S1070328418090075

INTRODUCTION

Recently, the design and assembly of coordination polymers (CPs) has become an area of rapid growth not only owing to their potential applications as functional materials in the fields of gas separation, ion exchange, luminescence, and heterogeneous catalysis, but also to their intriguing variety of molecular architectures and topologies [1–5]. It is well established that the choice of metal ions and organic ligands are crucial for the construction of coordination polymers. The flexibility, the number of ligand coordination sites, and metal ions are the main factors that influence the final network topology [1–8]. Usually, flexible or semirigid ligands allow them to rotate when coordinated to central metal ions. Therefore, a flexible or semirigid ligand make it possible to construct an entangled structure. Moreover, the coordination numbers of the central metals also can influence the final topologies of the coordination polymers.

In our previous works, we have successfully synthesized a series of coordination polymers using bidentate N-donor ligand bis(4-(1*H*-imidazol-1-yl)phenyl)methanone (Bipmo) [9–11]. As part of our research on coordination polymers with *N*-donor ligands, we reported here two CPs based on bidentate N-donor ligand Bipmo and organic carboxylates (Scheme 1), namely, $[Zn_2(Bipmo)_2(Adip)_2 \cdot 2H_2O]_n$ (**I**), $[Zn(Bipmo)(Adip) \cdot 2H_2O]_n$ (**II**) (H_2Adip = adipic acid). The complexes were characterized by X-ray crystallography, elemental analyses, IR spectra and thermogravimetric (TG) analyses. The effects of ligand linker and central metals on the final topologies have been discussed in detail. In addition, the luminescent properties of the bipmo and compounds **I**, **II** have also been investigated.

[1] The article is published in the original.

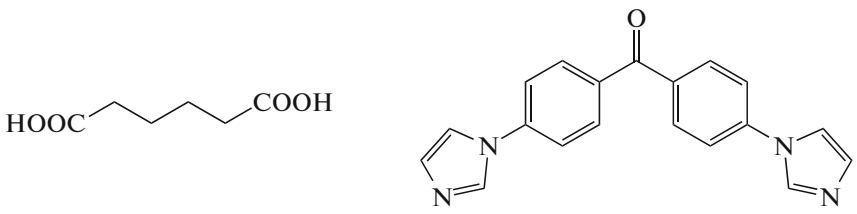

H_2Adip Bipmo

Scheme 1.

EXPERIMENTAL

Materials and measurements. All solvents, $Zn(Ac)_2 \cdot 2H_2O$, $Cd(Ac)_2 \cdot 2H_2O$, and adipic acid were purchased from commercial sources and used without further purification. Ligand Bipmo was synthesized according to the literature [9]. Elemental analyses (EA) were performed on an Elementar Vario ELIII elemental analyzer. The IR spectra were recorded on a Bruker Vector 22 spectrophotometer with KBr pellets in the 4000–400 cm^{-1} region. The Luminescence spectra were measured on a Hitachi F-4600 fluorescence spectrometer. TG analyses were carried out on a NETZSCH STA 449F3 unit at a heating rate of 10°C min^{-1} in air.

Synthesis of complexes I and II. A mixture of $Zn(Ac)_2 \cdot 2H_2O$ (21.9 mg, 0.1 mmol), Bipmo (31.4 mg, 0.1 mmol), and H_2Adip (14.6 mg, 0.1 mmol) was dissolved in 6 mL of DMF–H_2O (1 : 1, v/v). The final mixture was placed in a Parr Teflon-lined stainless-steel vessel (15 mL) under autogenous pressure and heated at 105°C for 7 days. Colorless block single crystals **I** and yellow single crystals suitable for X-ray data collection were obtained by filtration, washed with H_2O and air-dried.

I: Yield was 46% (colorless, based on Bipmo).

IR (KBr; ν, cm^{-1}): 3120 m, 3059 w, 2925 w, 2079 w, 1667 s, 1622 s, 1516 s, 1493 m, 1478 w, 1387 m, 1307 m, 1276 m, 1240 m, 1199 w, 1125 m, 1061 m, 963 w, 943 w, 926 m, 875 w, 862 w, 767 w, 744 m, 674 m, 660 m, 470 w.

For $C_{25}H_{24}N_4O_6Zn$

Anal. calcd., %	C, 55.41	H, 4.46	N, 10.34
Found, %	C, 55.23	H, 4.35	N, 10.46

II: Yield was 26% (yellow, based on Bipmo).

IR (KBr; ν, cm^{-1}): 3147 m, 2952 w) 2927 w, 2859 w, 2079 w, 1638 s, 1618 s, 1525 s, 1498 s, 1457 m, 1414 m, 1335 m, 1309 m, 1286 m, 1255 m, 1186 m, 1128 w, 1060 w, 964 w, 945 w, 930 w, 852 w, 764 w, 667 w, 649 m, 623 m, 512 w, 478 w, 410 w.

For $C_{25}H_{26}N_4O_7Zn$

Anal. calcd., %	C, 53.63	H, 4.68	N, 10.01
Found, %	C, 53.49	H, 4.59	N, 10.18

X-ray crystallographic studies. X-ray crystallographic data of **I**, **II** were recorded on an Agilent Technology SuperNova Eos Dual system with a (MoK_α, $\lambda = 0.71073$ Å) micro focus source and focusing multilayer mirror optics. The data were collected at a temperature of 293 K and processed using CrysAlis^{Pro} [12]. The structures were solved by direct methods [13] with the SHELXTL (version 6.10) program [14] and refined by full matrix least-squares techniques on F^2 with the SHELXTL [14]. All non-hydrogen atoms were refined anisotropically and the hydrogen atoms bonded to carbon atoms were generated geometrically. The water hydrogen atoms were first located in the difference map then positioned geometrically and allowed to ride on their respective parent atoms. Crystallographic data and structure refinements for compounds **I**, **II** are listed in Table 1. Selected bond distances and angles for **I**, **II** are summarized in Table 2.

Supplementary material for structures has been deposited with the Cambridge Crystallographic Data Centre (CCDC nos. 1555292 (**I**), 1555289 (**II**); deposit@ccdc.cam.ac.uk or http://www.ccdc.cam.ac.uk).

RESULTS AND DISCUSSION

Complexes **I**, **II** were prepared from the reaction with $Zn(Ac)_2 \cdot 2H_2O$, Bipmo, and H_2Adip in a 1 : 1 : 1 molar ratio under solvothermal conditions. They were characterized by IR, EA, TG, and single-crystal X-ray analyses. The coordination polymers **I**, **II** consist of both the Bipmo ligand and carboxylate anions. In order to investigate the topologies of the resulting frameworks of the bipmo ligand with Zn(II) salts and different polycarboxylates, we carried out numerous parallel experiments by adjusting the ratios of the reaction materials. In addition, we also performed a series of parallel experiments to change the reaction temperatures, and to vary the solvent types and ratios. However, other experiments gave powder forms or very small polycrystals.

In structure **I**, Zn atom lies on a double crystallographic axis. As shown in Fig. 1a, the asymmetric unit of **I** contains one Zn^{2+} ion, one $Adip^{2-}$ anion, one Bipmo ligand and a lattice water molecule. The Zn^{2+} ion is four-coordinated by two carboxylate O atoms

from two $Adip^{2-}$ anions and two N atoms from two Bipmo ligands in a tetrahedral geometry. The Zn(1)–O(1) and Zn(1)–N(1) bond lengths are 1.9466(15) Å and 2.0232 Å, respectively.

Each carboxylate group of the $Adip^{2-}$ coordinates with one Zn(II) atom in a monodentate coordination mode. In this way, the $Adip^{2-}$ anions bridge adjacent Zn(II) atoms to generate a 1D chain. Neighboring chains are further linked by Bipmo ligands in *cis*, *trans* conformations to furnish a 2D wave-like structure with (4,4) topology (Fig. 1b). Interestingly, each layer is threaded by the adjacent layers from above and below layers, thus resulting in an unusual 2D → 2D polythreading motif involving 4-fold interpenetrating wave-like sheets (Fig. 1c), which interpenetrate in a 2D → 2D parallel manner and pillar to generate 3D architectures (Fig. 1d).

The asymmetric unit of **II** contains one Zn^{2+} ions, one Bipmo ligand, one deprotonated H_2Adip ligands and two lattice water molecules. As shown in Fig. 2a, each Zn^{2+} ion is four-coordinated with a slightly distorted $\{ZnN_2O_2\}$ tetrahedral coordination geometry, which is coordinated by two nitrogen atoms from two bipmo ligands, two oxygen atoms from two deprotonated $Adip^{2-}$ ligands. The Zn(1)–N(1), Zn(1)–$N(4)^{\#2}$, Zn(1)–O(1), and Zn(1)–$O(4)^{\#1}$ bond lengths are 2.002(3), 2.026(3), 1.936(3), and 1.947(3) Å, respectively ($^{\#1}$ x, $-y$, $z - 1/2$; $^{\#2}$ $x + 1/2$, $y + 1/2$, $z + 1$), which are similar to the reported values for Zn–O (1.910(3)–2.276(6) Å) and Zn–N (1.973(7)–2.168(4) Å) [15–17].

The deprotonated carboxylic groups of H_2Adip ligand adopting μ^1-η^1:η^0 coordination mode link Zn^{2+} ions to form a 1D chain. These adjacent 1D chains are connected by adjacent Bipmo ligands to yield a 3D network (Fig. 2b). Topologically, both $Adip^{2-}$ and Bipmo ligands serve as the 2-connected spacers, and each Zn^{2+} ion is 4-connected. Thus, the overall 3D network shows a 2-fold interpenetrated 4-connected 3D Cds network with a point symbol of (6^5.8) (Figs. 2b, 2c).

Luminescent coordination polymers with d^{10} metal atoms are currently attracting much interest for their various functionalities and applications in photocatalysis, fluorescentsensors, biomedical imaging, and electroluminescent devices [18–21]. The luminescent properties of the Bipmo ligand (**I** and **II**) have been investigated in the solid state at room temperature (Fig. 3). The main emission peak of the free Bipmo ligand is at 447 nm (λ_{ex} = 407 nm), which may be attributed to the $\pi^* \rightarrow n$ or $\pi^* \rightarrow \pi$ transitions [22]. Complexes **I**, **II** show broad emission bands with the maximum peak at 494 nm (λ_{ex} = 376 nm) for **I**, 505 nm (λ_{ex} = 372 nm) for **II**. Compared with free Bipmo

Table 1. Crystallographic data and refinement parameters for structures **I** and **II**

Temperature, K	293(2)	293(2)
Fw	1083.74	559.89
Crystal system	Monoclinic	Monoclinic
Crystal size, mm	0.28 × 0.27 × 0.25	0.27 × 0.21 × 0.18
Space group	*C*2/*c*	*C*2/*c*
a, Å	8.2385(4)	25.6046(19)
b, Å	27.1500(11)	13.3254(9)
c, Å	11.0763(7)	19.1687(11)
β, deg	110.556(6)	127.342(4)
V, Å^3	2319.8(2)	5199.6(6)
ρ_{cacld}, g cm^{-3}	1.552	1.430
Z	2	8
μ, mm^{-1}	1.110	0.995
θ Range, deg	3.00–25.10	2.96–25.19
Reflections measured/unique (R_{int})	4392/2064 (0.0314)	12238/4672 (0.0209)
Reflections with $I > 2\sigma(I)$	1913	3618
Data/restraints/parameters	2064/0/165	4672/0/334
GOOF on F^2	1.027	1.075
R_1, wR_2 ($I > 2\sigma(I)$)	0.0310, 0.0750	0.0555, 0.1681
R_1, wR_2 (all data)	0.0340, 0.0769	0.0683, 0.1782
$\Delta\rho_{max}/\Delta\rho_{min}$, *e*/Å^3	0.244/–0.353	0.598/–0.511

Table 2. Selected bond lengths and angles for complex **I** and **II***

Bond	*d*, Å	Bond	*d*, Å
		I	
C(7)–N(2)	1.434(3)	O(1)–Zn(1)	1.9466(15)
C(13)–O(5)	1.220(4)	C(1)–O(2)	1.225(3)
C(13)–C(10)$^{\#2}$	1.495(3)	C(1)–O(1)	1.292(3)
C(4)–N(1)	1.315(3)	C(3)–C(3)$^{\#1}$	1.510(4)
C(4)–N(2)	1.347(3)	C(5)–N(1)	1.373(3)
N(1)–Zn(1)	2.0232(17)	C(6)–N(2)	1.380(3)
		II	
Zn(1)–O(4)$^{\#1}$	1.947(3)	Zn(1)–N(4)$^{\#2}$	2.026(3)
Zn(1)–O(1)	1.936(3)	Zn(1)–N(1)	2.002(3)
C(1)–O(1)	1.240(6)	C(1)–O(2)	1.243(6)
C(6)–O(3)	1.225(5)	C(16)–O(5)	1.220(5)
C(6)–O(4)	1.277(5)	C(20)–N(3)	1.420(5)
C(7)–N(1)	1.309(4)	C(23)–N(4)	1.316(5)
C(7)–N(2)	1.340(5)	C(23)–N(3)$^{\#4}$	1.348(4)
C(8)–N(1)	1.371(5)	C(24)–N(4)	1.369(5)
C(9)–N(2)	1.381(4)	C(25)–C(24)$^{\#2}$	1.344(5)
C(10)–N(2)	1.434(4)	C(25)–N(3)	1.376(5)
Angle	ω, deg	Angle	ω, deg
		I	
O(2)C(1)O(1)	122.9(2)	C(4)N(1)Zn(1)	130.91(15)
O(2)C(1)C(2)	122.1(2)	C(4)N(2)C(6)	106.92(18)
O(1)C(1)C(2)	114.92(19)	C(4)N(2)C(7)	128.64(18)
C(2)C(3)C(3)$^{\#1}$	113.8(2)	C(6)N(2)C(7)	124.32(18)
N(1)C(4)N(2)	110.55(19)	C(1)O(1)Zn(1)	117.08(14)
C(12)C(7)N(2)	118.47(19)	O(1)$^{\#3}$Zn(1)O(1)	98.99(9)
O(5)C(13)C(10)$^{\#2}$	119.76(13)	O(1)Zn(1)N(1)	111.51(7)
C(10)C(13)C(10)$^{\#2}$	120.5(3)	O(1)Zn(1)N(1)$^{\#3}$	114.74(7)
C(4)N(1)C(5)	106.57(18)	N(1)Zn(1)N(1)$^{\#3}$	105.64(10)
		II	
O(1)C(1)O(2)	122.4(4)	C(24)$^{\#2}$C(25)N(3)	106.9(3)
O(1)C(1)C(2)	117.3(4)	C(7)N(2)C(9)	106.4(3)
O(2)C(1)C(2)	120.3(5)	C(7)N(2)C(10)	126.2(3)
O(3)C(6)O(4)	121.7(4)	C(9)N(2)C(10)	127.1(3)
O(3)C(6)C(5)	121.1(4)	C(23)$^{\#2}$N(3)C(25)	106.8(3)
O(4)C(6)C(5)	117.2(4)	C(23)$^{\#2}$N(3)C(20)	125.2(3)
N(1)C(7)N(2)	111.5(3)	C(25)N(3)C(20)	128.1(3)
C(9)C(8)N(1)	110.7(3)	C(23)N(4)C(24)	106.8(3)
C(8)C(9)N(2)	106.3(3)	C(7)N(1)C(8)	105.1(3)
C(11)C(10)N(2)	120.7(3)	C(6)O(4)Zn(1)$^{\#3}$	111.2(3)
C(15)C(10)N(2)	119.1(3)	O(1)Zn(1)O(4)$^{\#1}$	109.26(16)
O(5)C(16)C(17)	119.0(4)	O(1)Zn(1)N(1)	115.21(14)
C(25)$^{\#4}$C(24)N(4)	109.0(4)	O(4)$^{\#1}$Zn(1)N(1)	110.85(14)
C(21)C(20)N(3)	120.5(3)	O(1)Zn(1)N(4)	97.09(14)
C(19)C(20)N(3)	120.3(3)	O(4)$^{\#1}$Zn(1)N(4)	117.13(14)
N(4)C(23)N(3)$^{\#4}$	110.5(3)	N(1)Zn(1)N(4)	106.86(12)

* Symmetry transformations used to generate equivalent atoms: $^{\#1}$ $-x-1, -y, -z+1$; $^{\#2}$ $-x+2, y, -z+3/2$; $^{\#3}$ $-x, y, -z+1/2$ (**I**); $^{\#1}$ $x, -y, z-1/2$; $^{\#2}$ $x+1/2, y+1/2, z+1$; $^{\#3}$ $x, -y, z+1/2$; $^{\#4}$ $x-1/2, y-1/2, z-1$ (**II**).

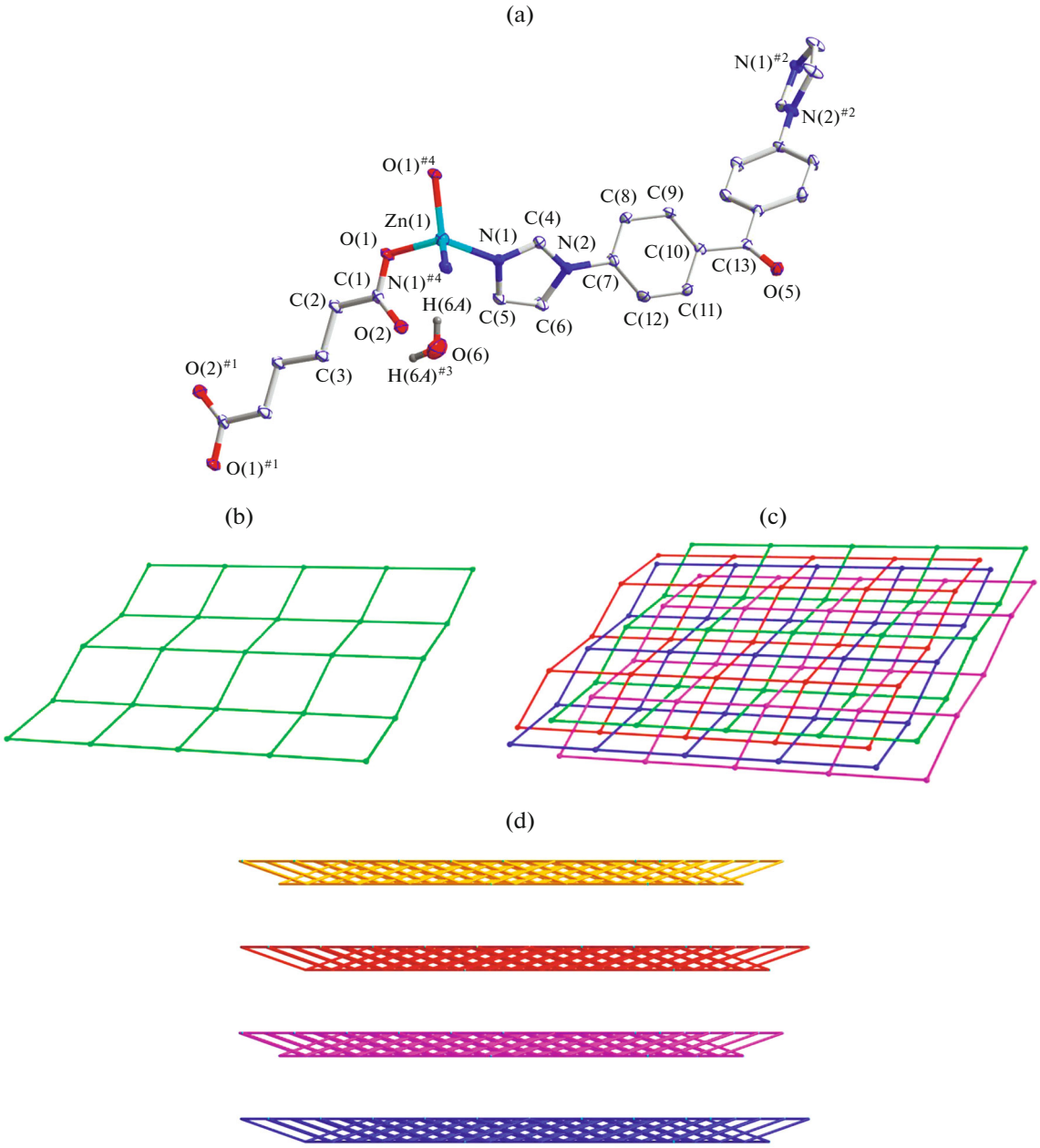

Fig. 1. Coordination environments of complex **I** (the hydrogen atoms bonded to carbon atoms are omitted for clarity, 30% ellipsoid probability, symmetry codes: #1 $-x-1, -y, -z+1$; #2 $-x+2, y, -z+3/2$; #3 $-x, y, -z+1/2$) (a); view of 4-fold interpenetrating 2D architecture of **I** (b); one of the 2D wave-like sheet (c); perspective view of the allignment of 4-fold interpenetrating layer of **I** (d).

ligand, the emissions for **I** and **II** are red-shifted by 47 and 58 nm, respectively, which may be assigned to metal-to-ligand charge transfer (MLCT), and similar red shifts have been reported before [22]. It is interesting that the complexes with the same Zn(II) center and N-donor ligand show different behaviors, which are probably attributed to the coordination environment around them and the structural topologies.

TG analyses of complexes **I**, **II** were carried out to investigate the thermal stabilities within the range of 30 to 800°C in air (Fig. 4). For complex **I**, the weight loss corresponding to the release of free water molecules is observed from 82 to 281°C (obsd. 3.51%, calcd. 3.33%). It continues to decompose upon further heating and undergoes a slow weight loss of 27.52% covering the temperature from 281 to 385°C, which corresponds to the destruction of Adip (calcd.

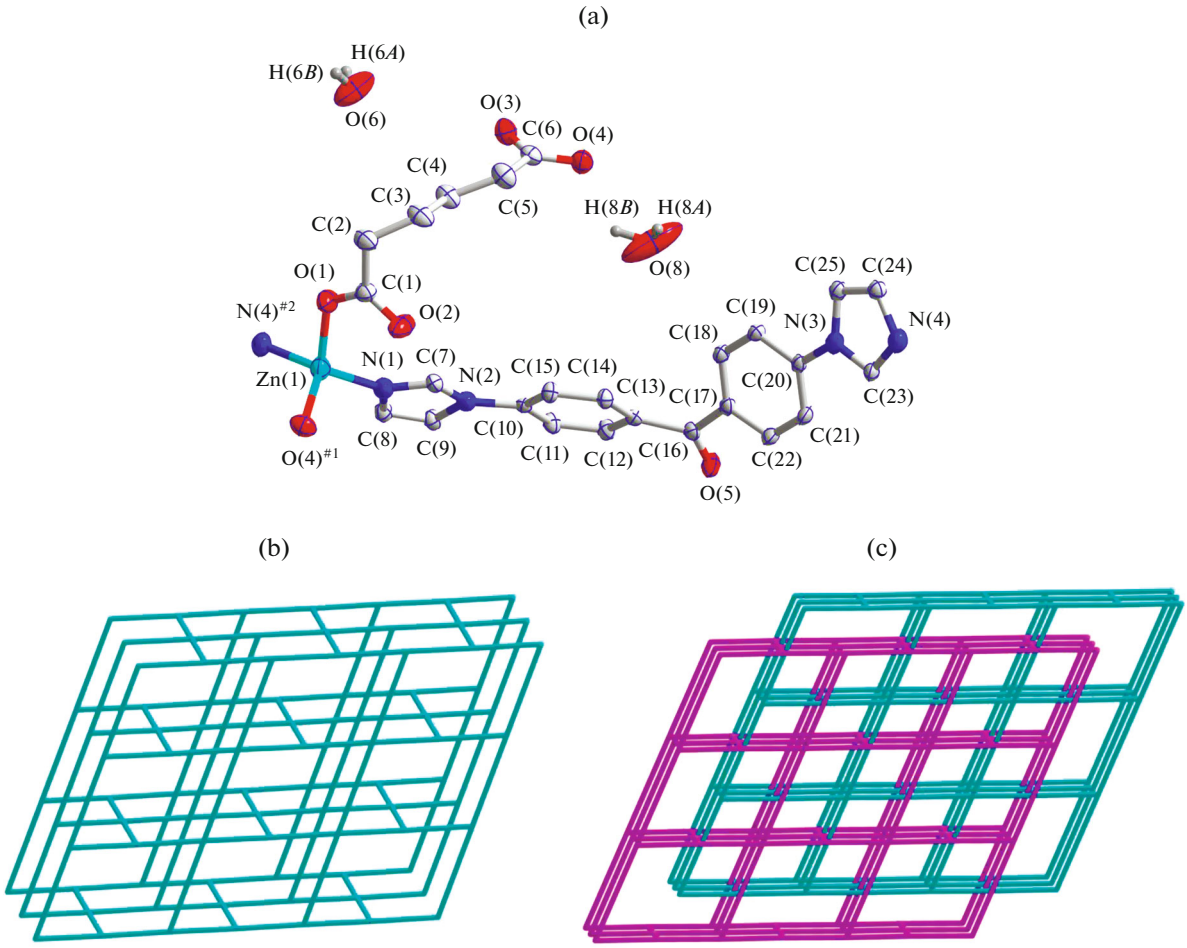

Fig. 2. Coordination environments of complex **II** (the hydrogen atoms bonded to carbon atoms are omitted for clarity, 30% ellipsoid probability, symmetry codes: #1 *x*, –*y*, *z* – 1/2; #2 1/2 + *x*, 1/2 + *y*, 1 + *z*) (a); one of the 3D net structure (b); topological view of compound **II** having two-fold interpenetrated 4-c uninodal net structure (c).

26.62%). Then an advanced degradation process takes place after 498°C. The weight loss of 54.36% in the region of 498–543°C corresponds to the collapse of the Bipmo ligand (calcd. 58.04%). Finally, a plateau region is observed from 543 to 780°C. The remaining weight corresponds to the formation of zinc oxide (obsd. 14.61%, calcd. 14.97%).

Complex **II** exhibits an initial weight loss from 33 to 275°C, with the observed weight loss of 5.32% corresponding to the release of the coordinated water (obsd. 5.32%, calcd. 6.43%). After that, an additional weight loss of 26.31% up to 484°C is attributed to the gradual decomposition of the Adip ligand (calcd. 25.71%). It keeps losing weight from 484 to 535°C corresponding to the decomposition of the remaining group of Bipmo units (obsd. 54.51%, calcd. 56.07%). Finally, a plateau region is observed from 535 to 870°C. The final white residue is zinc oxide (obsd. 13.86%, calcd. 14.46%).

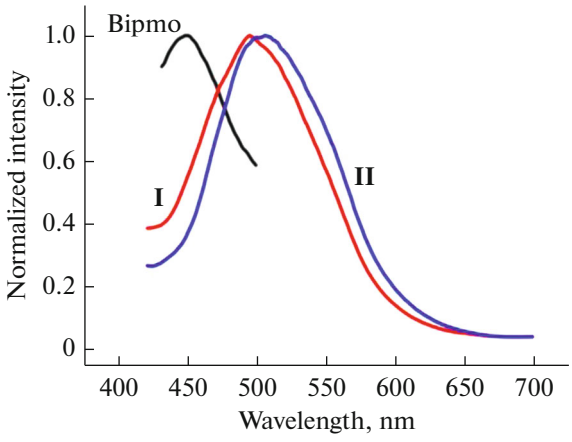

Fig. 3. Solid-state emission spectra of the Bipmo ligand, compounds **I**, **II** at room temperature.

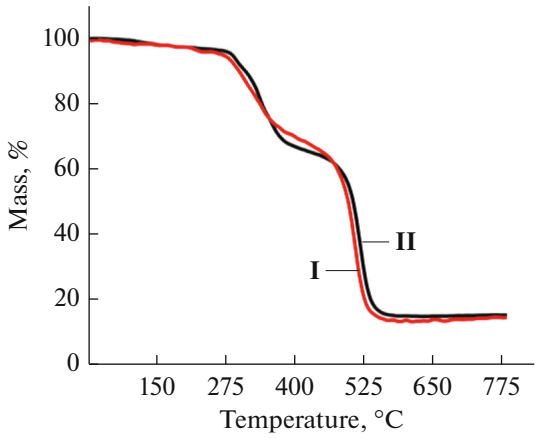

Fig. 4. The TG curves for complexes **I**, **II**.

In summary, two new Cds based on d^{10} metal ions, organic carboxylates, and Bipmo ligand have been synthesized under solvothermal conditions. The complexes show fascinating 2D and 3D structures. The multiple coordination sites and flexible nature of the ligands play a crucial role in the structural diversity. In addition, their luminescent behavior indicates that their different interpenetrating nets have subtle influences on the photoluminescent properties.

ACKNOWLEDGMENTS

We are grateful for financial support from Young Teacher Starting-up Research of Yuncheng University (no. YQ-2015007).

REFERENCES

1. Corma, A. and Garcia, H., and Llabres i Xamena, F.X., *Chem. Rev.*, 2010, vol. 110, p. 4606.
2. Chen, L., Tan, K., Lan, Y.Q., et al., *Chem. Commun.*, 2012, vol. 48, p. 5919.
3. Stylianou, K.C., Warren, J.E., Chong, S.Y., et al., *Chem. Commun.*, 2011, vol. 47, p. 3389.
4. Swamy, S.I., Bacsa, J., Jones, J.T.A., et al., *J. Am. Chem. Soc.*, 2010, vol. 132, p. 12773.
5. Ingram, C.W., Liao, L., Bacsa, J., et al., *Cryst. Growth Des.*, 2013, vol. 13, p. 1131.
6. Zhang, X., Fan, L., Sun, Z., et al., *Cryst. Growth Des.*, 2013, vol. 13, p. 792.
7. Rao, K., P., Higuchi, M., Duan, J., et al., *Cryst. Growth Des.*, 2013, vol. 13, p. 981.
8. Wang, P., Fan, R.-Q., Yang, Y.-L., et al., *CrystEngComm*, 2013, vol. 15, p. 4489.
9. Wang, G.-F., Zhang, X., Sun, S.-W., et al., *Z. Naturforsch., B*: *J. Chem. Sci.*, 2016, vol. 71, p. 869.
10. Wang, G.-F., Zhang, X., Sun, S.-W., et al., *Z. Naturforsch., B*: *J. Chem. Sci.*, 2017, vol. 72, p. 257.
11. Wang, G.-F., Zhang, X., Liu, Z.-R., et al., *Z. Naturforsch., B*: *J. Chem. Sci.*, 2017, vol. 72, p. 83.
12. *CrysAlis^{Pro}, Version 1.171.35.19,* Santa Clara: Agilent Technologies Inc., 2011.
13. Sheldrick, G.M., *SHELXTL-97*, Göttingen: Univ. of Göttingen, 1997.
14. Sheldrick, G.M., *Acta Crystallogr., Sect. A: Found. Crystallogr.*, 2008, vol. 64, p. 112.
15. Gao, J.Y., Wang, N., Xiong, X.H., et al., *CrystEngComm*, 2013, vol. 15, p. 3261.
16. Chen, C.-X., Wei, Z.-W., Qiu, Q.-F., et al., *Cryst. Growth Des.*, 2017, vol. 17, p. 1476.
17. Cheng, P.C., Kuo, P.T., Liao, Y.H., et al., *Cryst. Growth Des.*, 2013, vol. 13, p. 623.
18. Che, C.M., Chao, H.Y., Miskowski, V.M., et al., *J. Am. Chem. Soc.*, 2001, vol. 123, p. 4985.
19. McGarrah, J.E., Kim, Y.J., Hissler, M., et al., *Inorg. Chem.*, 2001, vol. 40, p. 4510.
20. He, X., Lu, C.Z., and Yuan, D.Q., *Inorg. Chem.*, 2006, vol. 45, p. 5760.
21. Ouellette, W., Hudson, B.S., and Zubieta, J., *Inorg. Chem.*, 2007, vol. 46, p. 4887.
22. Shi, X., Zhu, G., Fang, Q., et al., *Eur. J. Inorg. Chem.*, 2004, vol. 2004, p. 185.